

Original Paper

# Galectin-3: A Cardiomyocyte Antiapoptotic Mediator at 24-Hour Post Myocardial Infarction

Suhail Al-Salam<sup>a</sup> Satwat Hashmi<sup>b</sup> Govindan S. Jagadeesh<sup>a</sup> Saeed Tariq<sup>c</sup>

<sup>a</sup>Department of Pathology, College of Medicine and Health Sciences, United Arab Emirates University, Al Ain, United Arab Emirates, <sup>b</sup>Department of Biological and Biomedical Sciences, Aga Khan University, Karachi, Pakistan, <sup>c</sup>Department of Anatomy, College of Medicine and Health Sciences, United Arab Emirates University, Al Ain, United Arab Emirates

## Key Words

Heart • Myocardial infarction • Galectin 3 • Apoptosis

## Abstract

**Background/Aims:** Galectin 3 (GAL-3) is a beta galactoside binding lectin that has different roles in normal and pathophysiological conditions. GAL-3 has been associated with heart failure and was linked to increased risk of death in a number of studies. GAL-3 was found to be up regulated in animal models of heart failure as well as myocardial infarction (MI). The objective of this study is to test if high GAL-3 after myocardial infarction has a protective role on the heart through its anti-apoptotic and anti-necrotic functions. **Methods:** Male C57B6/J mice and GAL-3 knockout (KO) mice were used for permanent ligation of the left anterior descending artery of the heart to create infarction in the anterior myocardium. Heart and plasma samples were collected 24 hours after the induction of MI and were used for immunohistochemistry, Tunnel procedure, electron microscopy and enzyme linked immunosorbent assay (ELISA). **Results:** Our results show that the significant increase in GAL-3 levels in the left ventricle at 24-hour following MI is associated with significant lower levels of pro-apoptotic proteins; cytochrome c, Bax, annexin V, cleaved caspase-3 and a higher levels of anti-apoptotic protein Bcl2 in GAL-3 wild MI group than GAL-3 KO group. We also have identified the anti-apoptotic activity of GAL-3 is mediated through a significant increase in Akt-1, NF kappa-B and beta-catenin proteins. In addition, we have identified the antiapoptotic activity is mediated through a significant lower levels of cathepsin-D protein. **Conclusion:** We conclude that the increased levels of GAL-3 at 24-hour following MI regulate antiapoptotic mechanisms in the myocardium that will shape the future course of the disease. We also identified that the anti-apoptotic mechanisms are likely mediated through interaction of GAL-3 with Akt-1, NF kappa-B, beta-catenin and cathepsin D proteins.

© 2020 The Author(s). Published by  
Cell Physiol Biochem Press GmbH&Co. KG

S. Al-Salam and S. Hashmi share first authorship and contributed equally to this work.

Dr. Suhail Al-Salam,  
MBChB, FRCPath

Department of Pathology, College of Medicine and Health Sciences, United Arab Emirates University,  
Al Ain PO Box 17666 (United Arab Emirates)  
Tel. +97137137464, Fax +97137671966, E-Mail suhaila@uaeu.ac.ae

## Introduction

Myocardial infarction (MI) is a complex process involving different mechanisms and pathways culminating in cardiac structural and contractile dysfunction [1]. Apoptosis is one of the mechanisms which mediates cardiac myocyte death during ischemic injury [2-7]. Hypoxia has been shown to be the proximate stimulus for myocyte apoptosis [8], and alone was able to induce apoptosis in primary cultures of neonatal and adult cardiac myocytes [9]. Apoptosis is a highly regulated process in which several regulatory proteins participate. It is the balance between these regulatory proteins that decides the fate of the cell. Bax, bcl-2, Caspase-3, and cytochrome c are some of these proteins related to apoptosis that have been studied in myocardial infarction [10]. Inhibition of apoptosis after MI has the potential to reduce infarct size and improve myocardial function. This necessitates identification of key regulatory molecules that mediate this mechanism.

Galectin-3 (GAL-3) is a beta galactoside binding lectin that has different roles in normal and pathophysiological conditions [11]. It has been associated with heart failure (HF) in recent years [12]. Increased level of GAL-3 was linked to recurrent HF and increased risk of death in a number of studies [13-16]. GAL-3 was found to be up-regulated in animal models of HF even before the development of HF [17] which makes it very interesting to find out what happens in the heart when GAL-3 levels are high after MI and before the development of HF symptoms and signs.

Previous studies have shown that GAL-3 is involved in apoptosis [18-21]. GAL-3 contains the anti-death Asp-Trp-Gly-Arg (NWGR) motif [7, 13] which is critical for its antiapoptotic function. The anti-apoptotic activity of GAL-3 was also demonstrated in peritoneal macrophages when those from GAL-3-deficient mice were more sensitive to apoptotic stimuli than those from control mice [18]. GAL-3 protects cells against apoptosis by working through different mechanisms which suggest that GAL-3 regulates the common apoptosis commitment step.

As our previous results show substantial increase in the GAL-3 levels in the cardiomyocytes, endothelial cells and neutrophil polymorphs in the heart as well as plasma at 24 hours post MI time point [19], we hypothesized that high GAL-3 at 24 hours post MI time has a protective role on the heart through its anti-apoptotic and anti-necrotic functions. We used male C57BL6 mice and GAL-3 KO mice with the same background strain to look for apoptotic and necrotic markers at 24-hour post myocardial infarction heart samples.

## Materials and Methods

### *Murine model of myocardial infarction*

Male C57B6/J mice ( $n=16$ ) and GAL-3 KO mice ( $n=16$ ) were divided into 24 hour MI group and sham operated groups. All experimental animal procedures are approved by the Animals Ethics Committee of the College of Medicine and Health Sciences, UAE University.

GAL-3 wild and KO mice (male, age: 12-16 weeks; wt: 20-25g) were anesthetized by an intraperitoneal injection of Phenobarbitone (70mg/kg). The mice were then intubated by transesophageal illumination using a modified 22-gauge plastic cannula and fixed on the operating pad in the supine position by taping all four extremities. The mice were connected to a mouse ventilator (Harvard apparatus Minivent Hugo Sachs Elektronik) which supplied room air supplemented with 100% oxygen (tidal volume 0.2 ml/min., rate 120 strokes/min). Rectal temperature was continuously monitored and maintained within 36-37°C using a heat pad. The lead II ECG (AD Instrument multi-channel recorder interfaced with a computer running Power lab 4/30 data acquisition software) was recorded from needle electrodes inserted subcutaneously. Myocardial infarction was induced in the mice by permanently occluding the left anterior descending coronary artery (LAD) as described earlier [20-22].

Briefly, the chest was opened with a lateral incision at the 4<sup>th</sup> intercostal space on the left side of the sternum. Then the chest wall was retracted for better visualization of the heart. With minimal manipulation, the pericardial sac was removed and the left anterior descending artery (LAD) was visualized with a

stereomicroscope (Zeiss STEMI SV8). An 8-0 ophthalmic silk suture was passed under the LAD and ligated 1mm distal to left atrial appendage. Occlusion was confirmed by observing immediate paleness of the left ventricle post ligation. An accompanying ECG recording showed characteristic ST-Elevation which further confirmed ischemia. The chest wall was then closed by approximating the third and fourth ribs with one or two interrupted sutures. The muscles were returned back to their original position and the skin closed with 4-0 prolene suture. The animal was gently disconnected from the ventilator and spontaneous breathing was seen immediately. Post operative analgesic (Butorphanol 2mg/kg, s/c, 6 hourly) was given at the end of the procedure. Sham- operated mice underwent exactly the same procedure described above, except that the suture passed under the LAD is left open and untied. According to the experimental protocol, mice were sacrificed 24 hours after induction of myocardial infarction. The hearts were washed in ice cold PBS, right ventricle and both atria dissected away and left ventricle was immediately frozen in liquid nitrogen and later stored in -80 °C freezer. Blood was also collected in EDTA vacutainers and centrifuged at 3000 RPM for 15 minutes. The plasma was collected, aliquoted and stored at -80°C until further analysis. Heart samples from the same time point following LAD ligation were fixed in 10% buffered formal-saline for 24 hours.

### *Protein extraction from samples*

Total protein was extracted from heart samples by homogenizing with lysis buffer and collecting the supernatant after centrifugation. For total tissue homogenate, the Left ventricular (LV) heart samples were thawed, weighed and put in cold lysis buffer containing 50mM Tris, 300mM NaCl, 1mM MgCl<sub>2</sub>, 3mM EDTA, 20mM β-glycerophosphate, 25mM NaF, 1% Triton X-100, 10%w/v Glycerol and protease inhibitor tablet (Roche Complete protease inhibitor cocktail tablets). The hearts were homogenized on ice by a homogenizer (IKA T25 Ultra Turrax). The samples were then centrifuged at 14000 RPM for 15 minutes at 4°C, supernatant collected, aliquoted and stored at -80°C until further analysis. Total protein concentration was determined by BCA protein assay method (Thermo Scientific Pierce BCA Protein Assay Kit).

### *Tissue Processing*

Hearts were excised, washed with ice-cold phosphate buffer saline (PBS), blotted with filter paper and weighed. Each heart was sectioned into coronal slices of 2mm thickness then cassetted and fixed directly in 10% neutral formalin for 24 hours, which was followed by dehydration in increasing concentrations of ethanol, clearing with xylene and embedding with paraffin.

### *Immunohistochemistry*

Five-um sections were deparaffinized with xylene and rehydrated with graded alcohol. Sections were then placed in EnVision™ FLEX Target Retrieval Solution with a high PH (PH 9) (DAKO Agilent, USA) in a water bath at 95°C for 30 minutes. Sections were then washed with distilled water for 5 minutes followed by PBS for 5 minutes. Sections were then treated with peroxidase block for 30 minutes followed by protein block for 30 minutes. Sections were then incubated for one hour at room temperature with anti-cytochrome C antibody (rabbit monoclonal antibody 1:250, Cell Signaling Technology, USA), anti-Bcl2 antibody (Rabbit Polyclonal, 1:100, Abcam, USA), anti-cleaved caspase-3 antibody (Rabbit Polyclonal, 1:300, Cell signaling technology, USA), anti-Bax antibody (Rabbit Polyclonal, 1:100, Abcam, USA), anti-Wnt-3 antibody (Rabbit Polyclonal, 1:100, Abcam, USA), anti-beta-catenin antibody (Rabbit Polyclonal, 1:100, Abcam, USA), anti-Akt-1 antibody (Rabbit Polyclonal, 1:100, Santacruz biotechnology, USA), anti-phospho-NF kappa B antibody (Rabbit Polyclonal, 1:100, Abcam, USA). After conjugation with primary antibodies, sections were incubated with secondary antibody (EnVision™ Detection System, DAKO, Agilent, USA) for 20 minutes at room temperature followed by addition of DAB chromogen (EnVision™ Detection System, DAKO, Agilent, USA) and counter staining done with haematoxylin. Appropriate positive controls were used. For negative control, the primary antibody was not added to sections. Positive and negative controls were used in every batch of stained slides (not shown in figures).

### *Immunofluorescent labeling*

Five-um sections were deparaffinized with xylene and rehydrated with graded alcohol. Sections were placed in EnVision™ FLEX Target Retrieval Solution with a high PH (PH 9) (DAKO Agilent, USA) in a water bath at 95°C for 30 minutes. Sections were washed with distilled water for 5 minutes followed by PBS for 5 minutes. Sections were then incubated with anti-annexin-V antibody (Rabbit Polyclonal, 1:100, Abcam,

USA), overnight at room temperature. Sections were subsequently incubated with donkey anti-rabbit Alexa Fluor 488, (Jackson Immune Research Laboratories, USA, 1:100) antibody. Finally, sections were mounted in Dapi-water-soluble mounting media (Abcam, USA) and viewed with Olympus Fluorescent microscope. Appropriate positive control sections were used. For negative control, the primary antibody was not added to sections and the whole procedure carried out in the same manner as mentioned above. Positive and negative controls were used in every batch of stained slides (not shown in figures).

### *Tunnel Procedure*

*CardioTACS™ In Situ apoptosis detection kit (TREVIGEN<sup>®</sup> Helgerman CT, USA)* was used to detect apoptotic cells. Five-um sections were deparaffinised with xylene and rehydrated with graded alcohol. Sections were then placed in PBS for 10 minutes at room temperature. Sections were then covered with 50 µl of Proteinase K Solution and incubated for 30 minutes at room temperature, followed by washing for 2 times in deionized water, 2 minutes each. Sections were then immersed in Quenching Solution for 5 minutes at room temperature followed by washing for 1 minute at room temperature in deionized water to remove peroxide solution. Sections were then immersed in 1X TdT Labeling Buffer for 5 minutes. Sections were then covered with 50 µl of Labeling Reaction Mix and incubated at 37°C in humidity chamber for one hour. Sections were then immersed in 1X TdT Stop Buffer for 5 minutes at room temperature to stop labeling reaction. Sections were then washed 2 times in deionized water for 5 minutes each at room temperature. Sections were then covered with 50 µl of Streptavidin-HRP Solution and incubated at room temperature for 10 minutes. Sections were then washed in several changes of deionized water for 2 minutes each. Sections were then covered with 50 µl TACS™ Blue Label for 10 minutes. Sections were then immersed for 5 minutes in Nuclear Fast Red followed by washing in deionized water. Sections were then air dried and dehydrated with dipping ten times in 95% ethanol and cleared with two changes of p-xylene and mounted with a mounting medium.

### *Morphometric analysis*

Morphometric analysis of cytochrome c, Bcl2, cleaved caspase-3, Bax, annexin V, Akt-1, phospho-NFK-B, Wnt-3, and Beta-Catenin expression in left ventricular cells was done at 24 hours following MI using ImageJ software (<http://rsbweb.nih.gov/ij/>). In addition, apoptotic cells in the left ventricle at 24 hours MI detected by cardioTACS in situ tunnel procedure were also analyzed using ImageJ software (<http://rsbweb.nih.gov/ij/>).

Cytochrome c, Bcl2, cleaved caspase-3, Bax, annexin V, Akt-1, NFK-B, Wnt-3, and Beta-Catenin labeling were determined by counting the number of positive cells in randomly-selected high power fields (HPF) in the left ventricle. The mean numbers of positive cells will be converted from per HPF to per mm<sup>2</sup> (Each mm<sup>2</sup>= 4HPF). In addition, apoptotic cells labeling by cardioTACS in situ tunnel procedure were determined by counting the number of positive cells in randomly-selected high power fields (HPF) in the left ventricle. The mean numbers of positive cells will be converted from per HPF to per mm<sup>2</sup> (Each mm<sup>2</sup>= 4HPF).

For, cytochrome c, cleaved caspase-3, Bax, Akt-1, and Wnt-3, labeling, cells were considered positive when there was a cytoplasmic staining pattern. For annexin V labeling, cells were considered positive when there was a membranous/cytoplasmic staining patterns. For phospho-NFK-B and Beta-Catenin labeling, cells were considered positive when there was a nuclear staining pattern.

For apoptotic cells labeled by cardioTACS in situ tunnel procedure, cells were considered positive when there was a nuclear staining pattern.

### *Electron microscopic study*

Samples were immediately immersed in McDowell and Trump fixative for 3 h at 25°C. Tissues were then rinsed with ethanol and propylene oxide, infiltrated, embedded in Agar-100 epoxy resin, and polymerized at 65°C for 24 hours. Blocks were then trimmed and semithin and ultrathin sections were cut with Reichert Ultracuts, ultramicrotome. The semithin sections (1 µm) were stained with 1% aqueous toluidine blue on glass slides. The ultrathin sections (95 nm) on 200 mesh Cu grids were contrasted with uranyl acetate followed by lead citrate double stain. The grids were examined and photographed under a Tecnai G2 Spirit BioTwin transmission electron microscope.

*Enzyme linked immunosorbent assay*

Left ventricular myocardial concentration of cleaved caspase-3, Wnt-3a, Beta-Catenin, Phospho-NF kappa-B, Akt-1, and Cathepsin D were determined using enzyme linked immunosorbent assay (ELISA) development kits: mouse cleavedcaspase-3 [(DYC 835), R&D Systems, Minneapolis, MN, USA], mouse Wnt-3a [(DY1324B-05), R&D Systems, Minneapolis, MN, USA], mouse Beta-Catenin [(ab205704), Abcam, USA], Phospho-NF kappa-B [(ab176663), Abcam, USA], mouse Akt-1 [(DYC1775-2), R&D Systems, Minneapolis, MN, USA], and mouse Cathepsin D, [(ab239420), Abcam, USA] for sandwich ELISA, using standard procedure according to the manufacturer's instructions. The levels were normalized to total protein concentrations.

Briefly, 96-well plates (Nunc-Immuno Plate MaxiSorp Surface (NUNC Brand Products, A/S, Roskilde, Denmark), were coated with antibody specific to our proteins of interest. Biotinylated detection antibody and streptavidin conjugated horseradish peroxidase were used for detection of captured antigens. The plates between steps were aspirated and washed 3 times using ELISA plate washer (BioTek ELx50). Captured proteins were visualized using tetramethylbenzidine (TMB)/hydrogen peroxide. Absorbance readings were made at 450 nm, using a 96-well plate spectrophotometer (BioTek ELx800). Concentrations in the samples were determined by interpolation from a standard curve. Standards and samples were assayed in duplicate.

*Statistical analysis*

All statistical analyses were done using GraphPad Prism Software version 5. Comparisons between the various groups were achieved by one-way analysis of variance (ANOVA), followed by Newman-Keuls multiple range tests. Data are presented in mean ± standard error (S.E). P values < 0.05 are considered significant.

**Results**

*Antiapoptotic activity of Galectin-3 at 24 hour post MI*

*Cleaved Caspase 3 Activity.* Cleaved Caspase-3 activity was measured by ELISA in tissue homogenate of LV at 24-hour post MI hearts in the wild type and GAL-3 KO mice. Our results show a significant increase in cleaved caspase-3 in the LV of both GAL-3 wild and KO groups when compared to their sham control groups. Our results also show cleaved caspase-3 level is significantly higher in GAL-3 KO MI group than GAL-3 wild MI group ( $30700 \pm 820.6$  vs  $26380 \pm 1671$  pg/mg,  $p < 0.05$ ) (Fig. 1). Immunohistochemical staining of heart tissue sections showed a granular cytoplasmic and nuclear expression of cleaved caspase-3 in apoptotic cells in the area of infarction in both the GAL-3 wild and GAL-3 KO MI groups. The number of apoptotic cells that express cleaved Caspase-3 was significantly higher in GAL-3 KO MI group than GAL-3 wild MI group ( $P < 0.001$ ) (Fig. 2J-L).

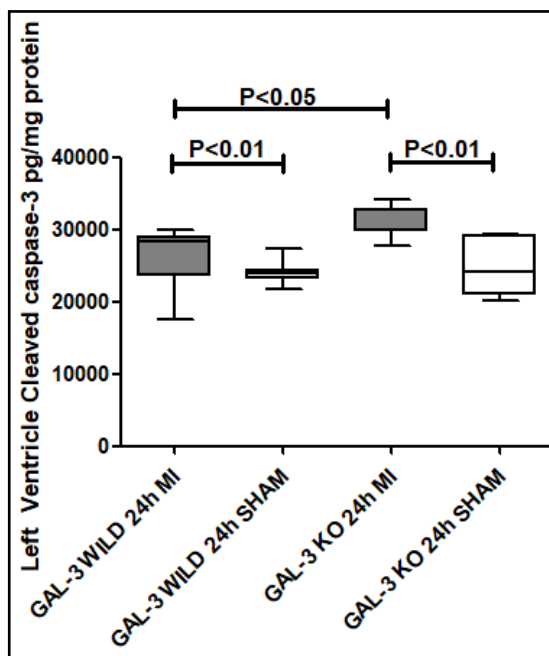
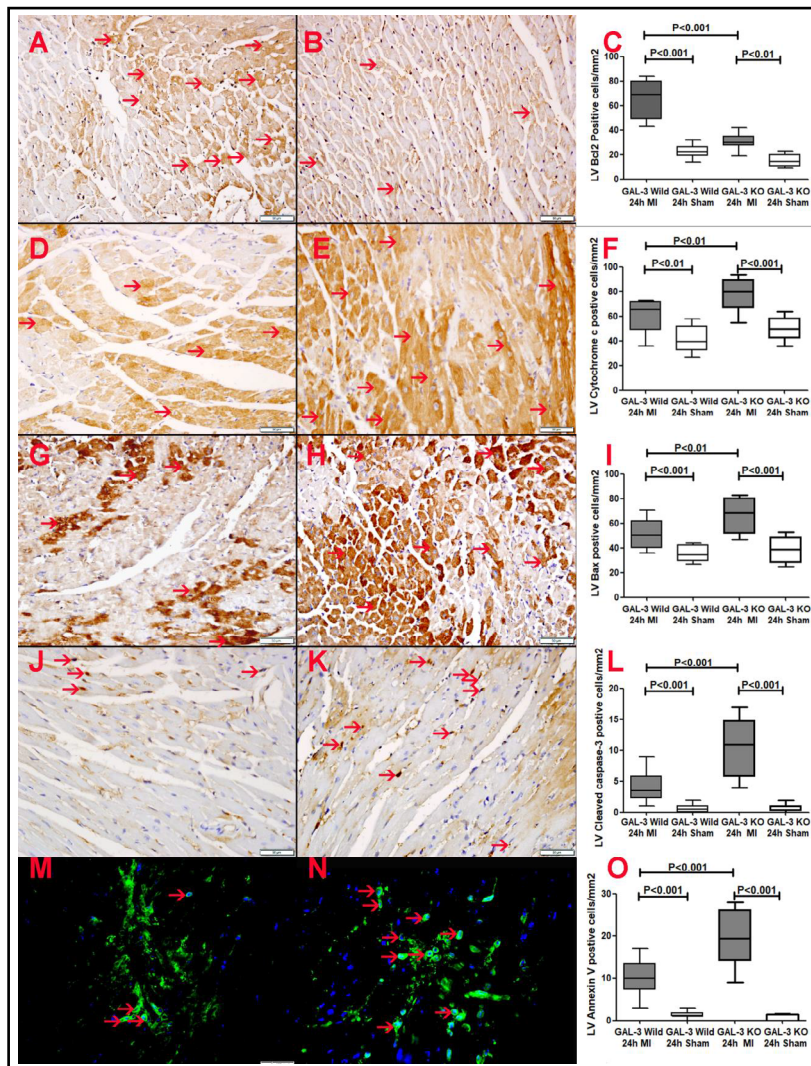


**Fig. 1.** The graph represents left ventricular Cleaved Caspase-3 at 24-hour post myocardial infarction in wild type C57BL6 and GAL-3 KO mouse heart. P value < 0.05 is statistically significant.

**Fig. 2.** Apoptotic and anti-apoptotic proteins in myocardial infarction. A. Representative section from the LV of GAL-3 wild MI group at 24-hour following MI showing cytoplasmic expression of Bcl2 by cardiomyocytes in the ischemic area (thin arrow). B. Representative section from the LV of GAL-3 KO MI group at 24-hour following MI showing cytoplasmic expression of Bcl2 by cardiomyocytes in the ischemic area (thin arrow). C. A morphometric graph showing a significantly higher number of cells expressing Bcl2 in the LV of GAL-3 wild MI group than GAL-3 KO MI group. D. Representative section from the LV of GAL-3 wild MI group at 24-hour following MI showing cytoplasmic expression of cytochrome c by cardiomyocytes in the ischemic area (thin arrow). E. Representative section from the LV of GAL-3 KO MI group at 24-hour following MI showing cytoplasmic expression of cytochrome c by cardiomyocytes in the ischemic area (thin arrow). F. A morphometric graph showing a significantly higher number of cells expressing cytochrome c in the LV of GAL-3 KO MI group than GAL-3 wild MI group. G. Representative section from the LV of GAL-3 wild MI group at 24h following MI showing cytoplasmic expression of Bax protein by cardiomyocytes in the ischemic area (thin arrow). H. Representative section from the LV of GAL-3 KO MI group at 24-hour following MI showing cytoplasmic expression of Bax protein by cardiomyocytes in the ischemic area (thin arrow). I. A morphometric graph showing a significantly higher number of cells expressing Bax protein in the LV of GAL-3 KO MI group than GAL-3 wild MI group. J. Representative section from the LV of GAL-3 wild MI group at 24-hour following MI showing cytoplasmic and nuclear expression of cleaved caspase-3 protein by apoptotic cells in the ischemic area (thin arrow). K. Representative section from the LV of GAL-3 KO MI group at 24-hour following MI showing cytoplasmic and nuclear expression of cleaved caspase-3 protein by apoptotic cells in the ischemic area (thin arrow). L. A morphometric graph showing a significantly higher number of cells expressing cleaved caspase-3 protein in the LV of GAL-3 KO MI group than GAL-3 wild MI group. M. Representative section from the LV of GAL-3 wild MI group at 24-hour following MI showing membranous expression of annexin V protein by apoptotic cells in the ischemic area (thin arrow). N. Representative section from the LV of GAL-3 KO MI group at 24-hour following MI showing membranous expression of annexin V protein by apoptotic cells in the ischemic area (thin arrow). O. A morphometric graph showing a significantly higher number of cells expressing Annexin V protein in the LV of GAL-3 KO MI group than GAL-3 wild MI group. Note: P value<0.05 is statistically significant.



**Bcl2 activity.** Immunohistochemical expression of Bcl2 protein was cytoplasmic and mainly seen in the cardiomyocytes. There was a significantly higher number of cells expressing Bcl2 protein in both GAL-3 wild ( $P<0.001$ ) and GAL-3 KO ( $P<0.01$ ) MI groups as compared to their sham control groups. There was a significant higher number of LV cardiomyocytes expressing Bcl-2 protein in GAL-3 wild type mice than GAL-3 KO mice ( $P<0.001$ ) (Fig. 2A-C).

**Cytochrome C activity.** Immunohistochemical expression of cytochrome c protein was cytoplasmic and mainly seen in the cardiomyocytes. There was a significantly higher number of cells expressing cytochrome c in both GAL-3 wild ( $P<0.01$ ) and GAL-3 KO ( $P<0.001$ ) MI groups as compared to their sham control groups. The number of LV cardiomyocytes expressing cytochrome c protein at 24-hour MI was also significantly higher in the GAL-3 KO mice than GAL-3 wild mice ( $P<0.01$ ) (Fig. 2D-F).

**Bax activity.** Immunohistochemical expression of Bax protein was cytoplasmic and mainly seen in the cardiomyocytes. There was a significantly higher number of cells expressing Bax protein in both GAL-3 wild ( $P<0.001$ ) and GAL-3 KO ( $P<0.001$ ) MI groups as compared to their sham control groups. The number of LV cardiomyocytes expressing Bax protein at 24-hour MI was also significantly higher in the GAL-3 KO mice than GAL-3 wild mice ( $P<0.01$ ) (Fig. 2G-I).

**Annexin V activity.** There was membranous staining of Annexin V to apoptotic cells in the LV at 24-hour MI. There was a significantly higher number of cells expressing annexin v in both GAL-3 wild ( $P<0.001$ ) and GAL-3 KO ( $P<0.001$ ) MI groups as compared to their sham control groups. There was also significantly higher number of cells stained with annexin V in GAL-3 KO mice as compared with GAL-3 wild mice ( $P<0.001$ ), (Fig. 2M-O).

**Tunnel Procedure.** Apoptotic cells show granular blue nuclear staining. There was a significantly higher number of apoptotic cells in both GAL-3 wild ( $P<0.001$ ) and GAL-3 KO ( $P<0.001$ ) MI groups as compared to their sham control groups. The number of apoptotic cells were significantly higher in GAL-3 KO MI group than GAL-3 wild MI group ( $P<0.01$ ) (Fig. 3).

**Cathepsin-D Activity.** Cathepsin D activity was measured by ELISA in the tissue homogenate of LV of 24 hour post MI hearts in GAL-3 wild and GAL-3 KO MI groups. There were significantly higher levels of cathepsin D protein in both GAL-3 wild ( $P<0.01$ ) and GAL-3 KO ( $P<0.001$ ) MI groups as compared to their sham control groups. Moreover, there was a significantly higher levels of cathepsin D in GAL-3 KO MI group ( $63.21 \pm 1.939$  pg/mg) than GAL-3 wild MI group ( $43.88 \pm 2.112$  pg/mg) ( $P<0.001$ ) (Fig. 4).

**Electron Microscopic study.** Ultrathin sections from cardiomyocytes of GAL-3 wild and GAL-3 KO MI mice show significant damage to mitochondria, rough endoplasmic reticulum, muscle fibrils, sarcolemmal membrane and nucleus in ischemic area at 24-hour following MI. An increased lysosomal activity was also seen however more lysosomes are seen in cardiomyocytes of GAL-3 KO MI group than GAL-3 wild MI group. There was increase in apoptotic bodies and cells in the myocardium at 24-hour MI. Examining ultrathin sections show a higher number of apoptotic bodies and cells in the myocardium of GAL-3 KO group than GAL-3 wild group (Fig. 5).

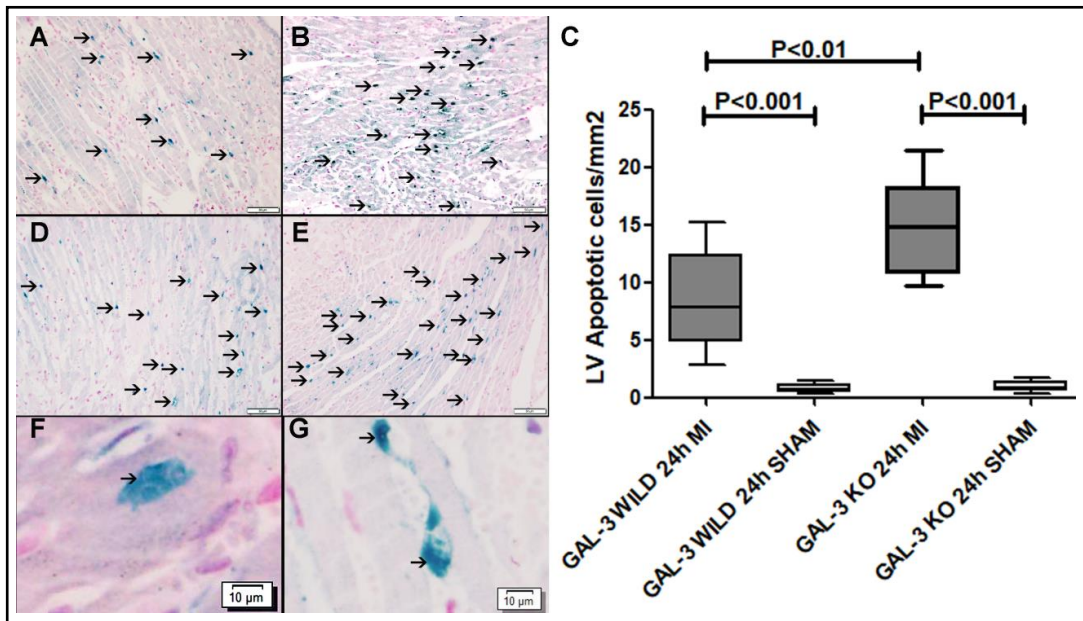


**Fig. 3.** CardioTACS™ In Situ apoptosis detection. A&C. Representative section from the LV of GAL-3 wild MI group at 24h following MI showing blue nuclear staining of apoptotic cells in the ischemic area (thin arrow). B&D. Representative section from the LV of GAL-3 KO MI group at 24-hour following MI showing blue nuclear staining of apoptotic cells in the ischemic area (thin arrow). E&F. A high power views show blue nuclear staining of apoptotic cardiomyocytes in the ischemic area (thin arrow). G. A morphometric graph showing a significantly higher number of blue-stained apoptotic cells in the LV of GAL-3 KO MI group than GAL-3 wild MI group, P value<0.05 is statistically significant.

**Fig. 4.** The graph represents left ventricular cathepsin D protein at 24-hour post myocardial infarction in wild type C57BL6 and GAL-3 KO mouse heart. P value<0.05 is statistically significant.

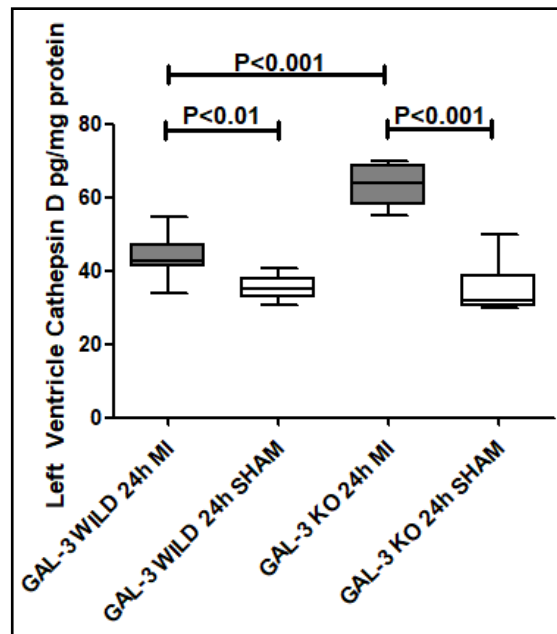
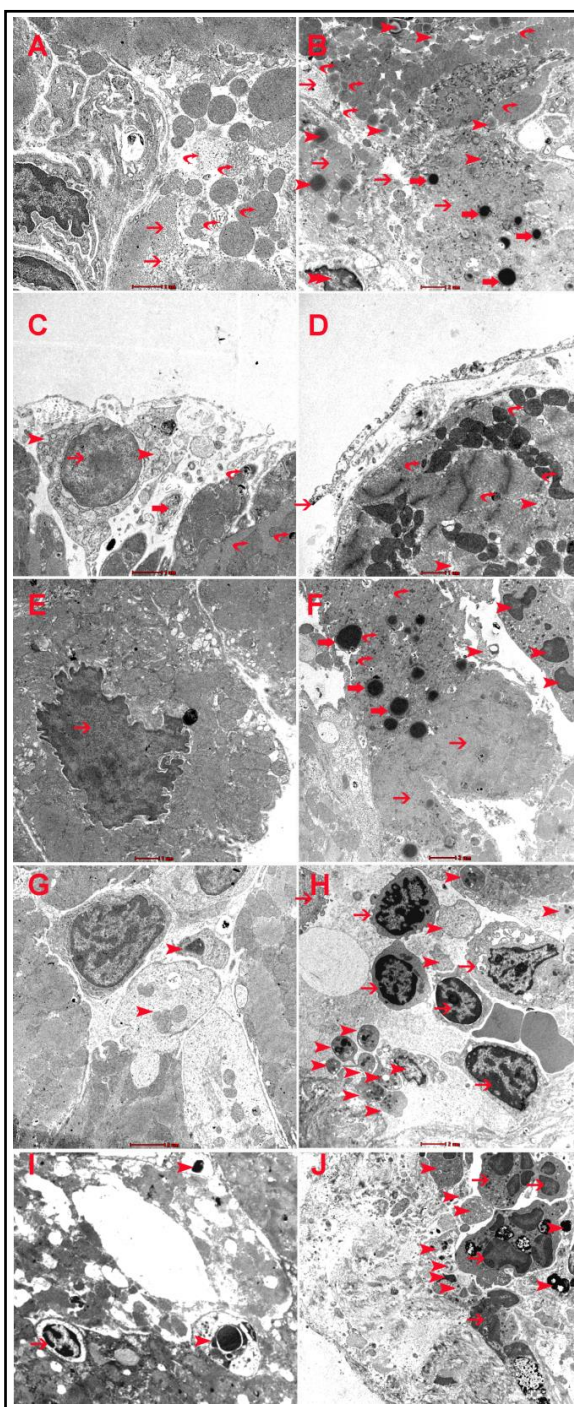


**Fig. 5.** Electron microscopic feature of cardiomyocytes at 24-hour following MI. A, C, E, G and I: Representative ultrathin section of cardiomyocyte from GAL-3 wild MI group showing A, damaged myofibrils (thin arrow) and damaged mitochondria (curved arrow). C, dilated rough endoplasmic reticulum (arrowhead), nuclear chromatin lysis (thin arrow), damaged microorganelle in a lysosome (thick arrow), and damaged mitochondria (curved arrow). E, Pyknotic nucleus with irregular nuclear membrane as early apoptotic nuclear changes in cardiomyocytes. G, two apoptotic bodies (arrowhead) and one apoptotic nuclear changes (thin arrow). I, apoptotic bodies (arrowhead) and one apoptotic nuclear changes (thin arrow). B, D, F, H and J: Representative ultrathin section of cardiomyocyte from GAL-3 KO MI group showing B, dilated rough endoplasmic reticulum (arrowhead), damaged mitochondria (curved arrow), lysosomes (thick arrow), damaged myofibrils (thin arrow), apoptotic cell (double arrowhead). D, damaged myofibrils (arrowhead), damaged mitochondria (curved arrow) and damaged sarcolemmal membrane (thin arrow). F, damaged myofibrils (arrowhead), damaged mitochondria (curved arrow), lysosomes (thick arrow), and apoptotic bodies (arrowhead). H, multiple apoptotic bodies (arrowhead) and apoptotic cells (thin arrow). J, multiple apoptotic bodies (arrowhead) and apoptotic cells (thin arrow).



#### Galectin-3 and Cell survival pathways

**Total Akt-1 and phospho-Akt activity.** Total Akt-1 protein was measured in LV tissue homogenates by ELISA and showed a significantly higher level in GAL-3 wild MI group when compared to sham control group ( $P < 0.01$ ), while GAL-3 KO MI group showed no significant difference from its sham control group. There was a significantly higher level of Akt-1 protein in GAL-3 wild MI group ( $2225 \pm 156.2$  pg/mg) than GAL-3 KO MI group ( $1816 \pm 84.76$  pg/mg), ( $P < 0.01$ ) (Fig. 6A).

In addition, heart sections stained for phospho-Akt showed a significantly higher number of stained cells in GAL-3 wild type than GAL-3 KO groups ( $P < 0.001$ ) (Fig. 7A-C).

**Phospho-NF Kappa-B.** Phospho-NF kappa-B protein was measured in LV tissue homogenates by ELISA and showed significantly higher levels in GAL-3 wild ( $P<0.001$ ) and GAL-3 KO ( $P<0.01$ ) MI groups as compared to their sham control groups. Moreover, there was a significantly higher levels of phospho-NF kappa-B in GAL-3 wild MI group ( $1.018 \pm 0.07133$  pg/mg) than GAL-3 KO MI group ( $0.7853 \pm 0.01795$  pg/mg) ( $P<0.001$ ), (Fig. 6B).

In addition, heart sections stained for phospho-NF Kappa-B showed a significantly higher number of nuclear-stained cells in GAL-3 wild type than GAL-3 KO groups ( $P<0.05$ ) (Fig. 7D-F).

**Wnt/beta-catenin pathway.** Beta-catenin protein was measured in LV tissue homogenates by ELISA and showed significantly higher levels in both GAL-3 wild ( $P<0.001$ ) and GAL-3 KO ( $P<0.01$ ) MI groups as compared to their sham control groups. Moreover, there was a significantly higher levels of beta-catenin protein in GAL-3 wild MI group ( $10.71 \pm 0.9369$  pg/mg) than GAL-3 KO MI group ( $8.635 \pm 0.2974$  pg/mg) ( $P<0.05$ ), (Fig. 6C).

In addition, heart sections stained for Beta-catenin protein showed a significantly higher number of nuclear-stained cells in GAL-3 wild type than GAL-3 KO groups ( $P<0.01$ ) (Fig. 7G-I).

## Discussion

GAL-3 has diverse functions depending upon its localization within the tissue. It may be extracellular, cytoplasmic or nuclear [23-26]. Understanding the precise function of GAL-3 in regulating different biological functions requires specific *in vivo* model systems [27]. Our model is a murine model of MI where the LV has undergone infarction and the LV as a whole is used to look for changes that may have occurred in both GAL-3 wild and KO hearts.

Previously we have shown that after 24 hours of permanent ligation of LAD, the LV tissue of GAL-3 wild mice showed a significant higher level of GAL-3 in MI group when compared with corresponding sham group and that it was being produced by cardiomyocytes, endothelial cells and neutrophils [19]. This significant increase prompted us to investigate the role of GAL-3 in relation to apoptosis and necrosis in the heart.

There are two major apoptotic pathways namely intrinsic and extrinsic pathway. Intrinsic apoptotic signaling causes cytochrome *c* release from the mitochondria. Cytochrome *c* in the cytosol initiates the formation of "apoptosome," which consists of cytochrome *c*, caspase adaptor proteins such as Apaf-1,

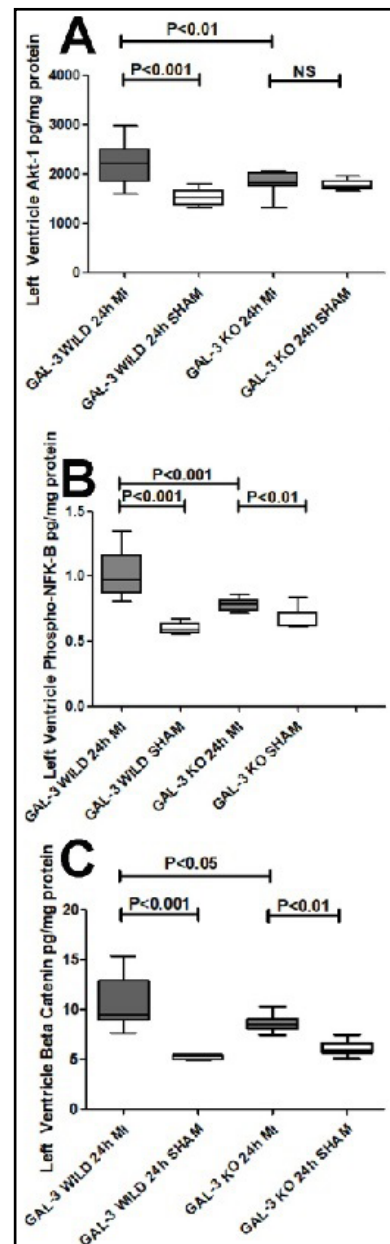


**Fig. 6.** A. The graph represents Total Akt-1 concentrations (pg/mg) at 24-hour post myocardial infarction in wild type C57BL6 and GAL-3 KO mouse heart. B. The graph represents phospho-NF kappa-B concentrations (pg/mg) at 24-hour post myocardial infarction in wild type C57BL6 and GAL-3 KO mouse heart. C. The graph represents beta-catenin concentrations (pg/mg) at 24-hour post myocardial infarction in wild type C57BL6 and GAL-3 KO mouse heart. Note: P value<0.05 is considered statistically significant.

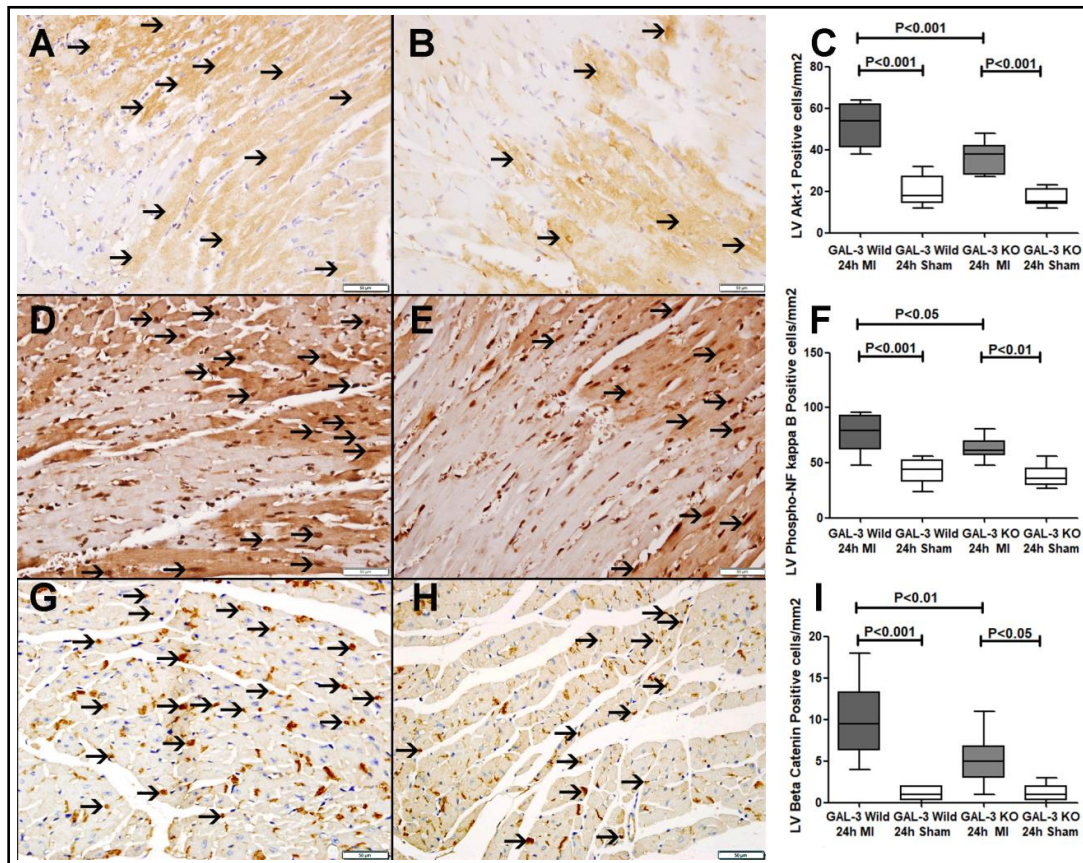


**Fig. 7.** A. Representative section from the LV of GAL-3 wild MI group at 24h following MI showing cytoplasmic expression of Akt-1 protein by cardiomyocytes in the ischemic area (thin arrow). B. Representative section from the LV of GAL-3 KO MI group at 24h following MI showing cytoplasmic expression of Akt-1 protein by cardiomyocytes in the ischemic area (thin arrow). C. A morphometric graph showing a significantly higher number of cells expressing Akt-1 protein in the LV of GAL-3 wild MI group than GAL-3 KO MI group. D. Representative section from the LV of GAL-3 wild MI group at 24h following MI showing nuclear expression of phospho-NF kappa-B protein by cardiomyocytes in the ischemic area (thin arrow). E. Representative section from the LV of GAL-3 KO MI group at 24h following MI showing nuclear expression of phospho-NF kappa-B protein by cardiomyocytes in the ischemic area (thin arrow). F. A morphometric graph showing a significantly higher number of cells with nuclear expression of phospho-NF kappa-B protein in the LV of GAL-3 wild MI group than GAL-3 KO MI group. G. Representative section from the LV of GAL-3 wild MI group at 24h following MI showing nuclear expression of beta-catenin protein by cardiomyocytes in the ischemic area (thin arrow). H. Representative section from the LV of GAL-3 KO MI group at 24h following MI showing nuclear expression of beta-catenin protein by cardiomyocytes in the ischemic area (thin arrow). I. A morphometric graph showing a significantly higher number of cells with nuclear expression of beta-catenin in the LV of GAL-3 wild MI group than GAL-3 KO MI group. Note: P value < 0.05 is statistically significant.

and caspases [28-30] and results in caspase activation, a commitment step for apoptosis induction. While, extrinsic apoptotic signals are mediated by cell-surface death receptors, including tumor necrosis factor, Fas and TRAIL receptor families. The death domains of the death receptor form the "death-inducing signaling complex," where caspases are activated.

The active or cleaved caspase- 3 acts on a number of death substrates that lead to the characteristic hallmarks of apoptotic cell; DNA and nuclear fragmentation, membrane blebbing and other morphological and biochemical alterations [31, 32].

Studies have shown that apoptosis can occur in cardiac myocytes after 3 hours of acute MI in mice [8], rats [33] and humans [34]. However, the exact mechanism is not completely clear.

GAL-3 has been found to be critically involved in apoptosis depending on its subcellular localization. Intracellular GAL-3 can inhibit apoptosis [35] whereas extracellular GAL-3 induces apoptosis [36]. Immunohistochemistry in our previous study [19], however, is showing intracellular localization of GAL-3. In this study we have examined the role of GAL-3 in apoptosis at 24-hour following MI, therefore, we have used GAL-3 KO mice to verify its role. Consequently, the post-MI antiapoptotic response was studied in the presence and absence of GAL-3.

Our results show that proapoptotic protein like cleaved caspase-3, Bax and cytochrome *c*, are significantly higher in the LV of GAL-3 KO MI group than GAL-3 wild MI group. We have also identified a significantly higher number of apoptotic cells expressing annexin v in the LV of GAL-3 KO group than GAL-3 wild type. In addition, tunnel procedure has shown a significant higher number of apoptotic cells in the LV of GAL-3 KO group than GAL-3 wild type. Electron microscopic examination of LV myocardium also shows a higher number of apoptotic bodies in GAL-3 KO MI group than GAL-3 wild MI group.

We have also checked anti apoptotic activity of Bcl-2 protein and found that its expression is considerably reduced in the LV of GAL-3 KO compared to GAL-3 wild type.

Our results are obviously showing the levels of studied LV proapoptotic and antiapoptotic proteins being significantly affected by the presence or absence of GAL-3, suggesting that at 24- hour post MI time, GAL-3 is controlling the apoptotic pathway by down regulating the proapoptotic proteins and increasing the anti-apoptotic Bcl-2. Literature has many reports regarding anti-apoptotic role of GAL-3. GAL-3 translocates to the perinuclear membrane following apoptotic stimuli [37, 38]. It is enriched in the mitochondria and prevents mitochondrial damage and cytochrome *c* release [35].

We have also shown a higher level of cathepsin D in the LV of GAL-3 KO MI group than GAL-3 wild MI group. Cathepsin D is a lysosomal protease expressed in all tissues and involved in nonspecific protein degradation in a strongly acidic environment of lysosomes [39].

Cathepsin D has been implicated in lysosome-related cell death [40]. It has been shown to control early processes in lysosome-mediated necrosis [41]. Lysosomes contribute to necrosis if complete lysosomal rupture occurs but also can drive apoptosis due to the release of cathepsins, into the cytosol as a consequence of lysosomal membrane permeabilization [42]. Porte Alcon et al. have shown increased Cathepsin D is involved in regulated necrosis [43]. Hence, the increased level of cathepsin D in tissue is usually seen in parallel with the cell death. Moreover, cathepsins have been widely implicated in apoptosis [44]. They are released into the cytosol as active enzymes where they can interact with a variety of apoptotic pathway substrates [45] which will contribute to caspase dependent and independent apoptosis with or without mitochondrial involvement [46]. Our finding of lower level of cathepsin D in the LV of GAL-3 wild MI group than GAL-3 KO MI group suggests a antiapoptotic role of GAL-3 at 24- hour MI.

GAL-3 has been linked to pro survival signal transduction pathways in previous studies. GAL-3 was shown to inhibit TNF- induced apoptosis through activation of Akt [45]. Also GAL-3 was found to enhance the PI3K/Akt activity, resulting in Tumor Necrosis Factor-Related Apoptosis-Inducing Ligand (TRAIL) resistance and inhibition of apoptosis [47]. Akt-1 is an anti-apoptotic protein, activated by phospholipid products of phosphatidylinositol 3-kinase (PI3K) and is a downstream target of PI3K in cell survival signaling [48]. We found significantly higher levels of total Akt-1 in the LV of GAL-3 wild MI group than GAL-3 KO MI group at 24-hour post MI. This supports the anti-apoptotic activity of GAL-3 being mediated through activation of Akt-1.

NF- $\kappa$ B is a transcription factor that plays important roles in regulating Inflammation, cell proliferation and cell survival. Phosphorylation plays a critical role in the activation of NF- $\kappa$ B downstream of all these stimuli [49]. NF- $\kappa$ B is now recognized as an important contributor to cell survival and protection from apoptosis [50, 51]. We have identified a significantly higher level of phosphorylated-NF kappa B in the LV in GAL-3 wild group than GAL-3 KO group. This is confirmed by higher nuclear stained cells with NF- $\kappa$ B in the LV at 24h MI

in GAL-3 wild group than GAL-3 KO mice. Interestingly, GAL-3 transcription under hypoxic conditions is triggered in an HIF-1 $\alpha$  and NF- $\kappa$ B dependent manner. Thus, overexpression of GAL-3 is part of an adaptive program leading to tumor cell survival under these stressful conditions [52]. Studies have shown NF- $\kappa$ B to be involved in the induction of GAL-3 [53] as well as GAL-3 is involved in the activation of NF- $\kappa$ B [54]. These findings suggest that the anti-apoptotic role of GAL-3 can also be mediated through activation of NF- $\kappa$ B.

The Wnt proteins has been shown to have protective effects on injured cells through its anti-apoptotic function via activation of  $\beta$ -catenin and c-Myc [55-57]. Wnt initiates canonical signaling by binding the Frizzled receptor and LRP co-receptor. This signals the phosphoprotein disheveled to traffic the destruction complex (Axin, CK1 $\alpha$ , APC, GSK-3 $\beta$ ) to the plasma membrane, allowing for translocation of  $\beta$ -catenin to the nucleus to activate transcription. GAL-3 has been found to be a novel binding partner of  $\beta$ -catenin [58]. We have shown an increase in the levels of  $\beta$ -catenin in the LV at 24-hour MI. We have also shown a significantly higher level of  $\beta$ -catenin in the LV of GAL-3 wild group than in GAL-3 KO group, which was confirmed by higher nuclear stained cells with  $\beta$ -catenin in the LV at 24-hour MI in GAL-3 wild group than GAL-3 KO mice, suggesting that GAL-3 can induce anti-apoptotic effect through activation of  $\beta$ -catenin. This finding is supported by work done by Song et al and Chen et al. which show Wnt signaling inhibits apoptosis by activating beta-catenin/T cell factor-mediated transcription [59, 60].

GAL-3 seems to link these pro survival signal transduction pathways investigated in our study. These pathways also have cross talk between them at various levels. For example, Wnt/ $\beta$ -catenin pathway players modulate many of their effects through interaction with NF- $\kappa$ B and reciprocally NF- $\kappa$ B also influences the Wnt/ $\beta$ -catenin signaling pathway [61], so it is understandable that GAL-3 is playing a central connector role in the pro survival signal transduction pathways.

Our study demonstrates that at 24-hour following MI the presence or absence of intracellular GAL-3 is associated with significant changes in proapoptotic and antiapoptotic proteins, and that the high GAL-3 levels in the myocardium is mediating an anti-apoptotic environment that may shape the future course of the disease. Anti-apoptotic mechanism in cardiomyocytes on one hand may be beneficial as it may protect the cardiomyocytes against death and prevent myocyte loss but on the other hand may prove to be deleterious as the rescued cardiomyocytes may not remain functional or may undergo necrosis later. Apoptosis may be viewed as a mechanism by which the heart limits the extent of a more destructive process of necrosis with its accompanying inflammation [8]. Inhibition of apoptosis in the neutrophil polymorphs can prolong their stay in the infarcted myocardium potentiating the effect of inflammation and destruction [62]. Apoptosis can therefore be considered a double-edged sword, which can work in either way.

Functional studies are very important, however, it was not our primary goal in this study and it will be considered in our future studies.

## Conclusion

We conclude that the increased levels of GAL-3 at 24-hour following MI regulate antiapoptotic mechanisms in the myocardium that will shape the future course of the disease. We also identified that the anti-apoptotic mechanisms are likely mediated through interaction of GAL-3 with Akt-1, NF kappa-B, Wnt3a, beta- catenin and cathepsin D proteins.

## Acknowledgements

The authors would like to thank The Zayed Bin Sultan Center for Health Sciences (Grant# 31R176), College of Medicine & Health Sciences, United Arab Emirates University for their support of this project. In addition, we would like to thank Ms Manjusha Sudhadevi from Department of Pathology, College of Medicine & Health Sciences, United Arab Emirates University, for her technical support.

## Disclosure Statement

The authors declare to have no competing interests.

## References

- 1 Ferdinandy P, Schulz R, Baxter GF: Interaction of cardiovascular risk factors with myocardial ischemia/ reperfusion injury, preconditioning, and postconditioning. *Pharmacol Rev* 2007;59:418-458.
- 2 Gottlieb RA, Bureson KO, Kloner RA, Babior BM, Engler RL: Reperfusion injury induces apoptosis in rabbit cardiomyocytes. *J Clin Invest* 1994;94:1621-1628.
- 3 Buerke M, Murohara T, Skurk C, Nuss C, Tomaselli K, Lefer AM: Cardioprotective effect of insulin-like growth factor I in myocardial ischemia followed by reperfusion. *Proc Natl Acad Sci U S A* 1995;92:8031-8035.
- 4 Itoh G, Tamura J, Suzuki M, Suzuki Y, Ikeda H, Koike M, Nomura M, Jie T, Ito K: DNA fragmentation of human infarcted myocardial cells demonstrated by the nick end labeling method and DNA agarose gel electrophoresis. *Am J Pathol* 1995;146:1325-1331.
- 5 Kajstura J, Cheng W, Reiss K, Clark WA, Sonnenblick EH, Krajewski S, Reed JC, Olivetti G, Anversa P: Apoptotic and necrotic myocyte cell deaths are independent contributing variables of infarct size in rats. *Lab Invest* 1996;74:86-107.
- 6 Fliss H, Gattlinger D: Apoptosis in ischemic and reperfused rat myocardium. *Circ Res* 1996;79:949-956.
- 7 Cheng W, Kajstura J, Nitahara JA, Li B, Reiss K, Liu Y, Clark WA, Krajewski S, Reed JC, Olivetti G, Anversa P: Programmed myocyte cell death affects the viable myocardium after infarction in rats. *Exp Cell Res* 1996;226:316-327.
- 8 Bialik S, Geenen DL, Sasson IE, Cheng R, Horner JW, Evans SM, Lord EM, Koch CJ, Kitsis RN: Myocyte apoptosis during acute myocardial infarction in the mouse localizes to hypoxic regions but occurs independently of p53. *J Clin Invest* 1997;100:1363-1372.
- 9 Tanaka M, Ito H, Adachi S, Akimoto H, Nishikawa T, Kasajima T, Marumo F, Hiroe M: Hypoxia induces apoptosis with enhanced expression of Fas antigen messenger RNA in cultured neonatal rat cardiomyocytes. *Circ Res* 1994;75:426-433.
- 10 Misao J, Hayakawa Y, Ohno M, Kato S, Fujiwara T, Fujiwara H: Expression of bcl-2 protein, an inhibitor of apoptosis, and Bax, an accelerator of apoptosis, in ventricular myocytes of human hearts with myocardial infarction. *Circulation* 1996;94:1506-1512.
- 11 Barondes SH, Cooper DN, Gitt MA, Leffler H: Galectins. Structure and function of a large family of animal lectins. *J Biol Chem* 1994;269:20807-20810.
- 12 Ho JE, Liu C, Lyass A, Courchesne P, Pencina MJ, Vasan RS, Larson MG, Levy D: Galectin-3, a marker of cardiac fibrosis, predicts incident heart failure in the community. *J Am Coll Cardiol* 2012;60:1249-1256.
- 13 van Kimmenade RR, Januzzi JL, Ellinor PT, Sharma UC, Bakker JA, Low AF, Martinez A, Crijns HJ, MacRae CA, Menheere PP, Pinto YM: Utility of amino-terminal pro-brain natriuretic peptide, galectin-3, and apelin for the evaluation of patients with acute heart failure. *J Am Coll Cardiol* 2006;48:1217-1224.
- 14 Lok DJ, Van Der Meer P, de la Porte PW, Lipsic E, Van Wijngaarden J, Hillege HL, van Veldhuisen DJ: Prognostic value of galectin-3, a novel marker of fibrosis, in patients with chronic heart failure: data from the DEAL-HF study. *Clin Res Cardiol* 2010;99:323-328.
- 15 de Boer RA, Lok DJ, Jaarsma T, van der Meer P, Voors AA, Hillege HL, van Veldhuisen DJ: Predictive value of plasma galectin-3 levels in heart failure with reduced and preserved ejection fraction. *Ann Med* 2011;43:60-68.

- 16 Lopez-Andrès N, Rossignol P, Iraqi W, Fay R, Nuée J, Ghio S, Cleland JG, Zannad F, Lacolley P: Association of galectin-3 and fibrosis markers with long-term cardiovascular outcomes in patients with heart failure, left ventricular dysfunction, and dyssynchrony: insights from the CARE-HF (Cardiac Resynchronization in Heart Failure) trial. *Eur J Heart Fail* 2012;14:74-81.
- 17 Sharma UC, Pokharel S, van Brakel TJ, van Berlo JH, Cleutjens JP, Schroen B, André S, Crijns HJ, Gabius HJ, Maessen J, Pinto YM: Galectin-3 marks activated macrophages in failure-prone hypertrophied hearts and contributes to cardiac dysfunction. *Circulation* 2004;110:3121-3128.
- 18 Hsu DK, Yang RY, Pan Z, Yu L, Salomon DR, Fung-Leung WP, Liu FT: Targeted disruption of the galectin-3 gene results in attenuated peritoneal inflammatory responses. *Am J Pathol* 2000;156:1073-1083.
- 19 Hashmi S, Al-Salam S: Galectin-3 is expressed in the myocardium very early post-myocardial infarction. *Cardiovasc Pathol* 24:213-223.
- 20 Michael LH, Entman ML, Hartley CJ, Youker KA, Zhu J, Hall SR, Hawkins HK, Berens K, Ballantyne CM: Myocardial ischemia and reperfusion: a murine model. *Am J Physiol* 1995;269:H2147-2154.
- 21 Michael LH, Ballantyne CM, Zachariah JP, Gould KE, Pocius JS, Taffet GE, Hartley CJ, Pham TT, Daniel SL, Funk E, Entman ML: Myocardial infarction and remodeling in mice: effect of reperfusion. *Am J Physiol* 1999;277:H660-668.
- 22 Hashmi S, Al-Salam S: Loss of dystrophin staining in cardiomyocytes: a novel method for detection early myocardial infarction. *Int J Clin Exp Pathol* 2013;6:249-257.
- 23 Moutsatsos IK, Davis JM, Wang JL: Endogenous lectins from cultured cells: subcellular localization of carbohydrate-binding protein 35 in 3T3 fibroblasts. *J Cell Biol* 1986;102:477-483.
- 24 Moutsatsos IK, Wade M, Schindler M, Wang JL: Endogenous lectins from cultured cells: nuclear localization of carbohydrate-binding protein 35 in proliferating 3T3 fibroblasts. *Proc Natl Acad Sci U S A* 1987;84:6452-6456.
- 25 Hubert M, Wang SY, Wang JL, Sève AP, Hubert J: Intranuclear distribution of galectin-3 in mouse 3T3 fibroblasts: comparative analyses by immunofluorescence and immunoelectron microscopy. *Exp Cell Res* 1995;220:397-406.
- 26 Openo KP, Kadrofske MM, Patterson RJ, Wang JL: Galectin-3 expression and subcellular localization in senescent human fibroblasts. *Exp Cell Res* 2000;25:278-290.
- 27 Henderson NC, Mackinnon AC, Farnworth SL, Poirier F, Russo FP, Iredale JP, Haslett C, Simpson KJ, Sethi T: Galectin-3 regulates myofibroblast activation and hepatic fibrosis. *Proc Natl Acad Sci U S A* 2006;103:5060-5065.
- 28 Cain K, Brown DG, Langlais C, Cohen GM: Caspase activation involves the formation of the aposome, a large (approximately 700 kDa) caspase-activating complex. *J Biol Chem* 1999;274:22686-22692.
- 29 Zou H, Henzel WJ, Liu X, Lutschg A, Wang X: Apaf-1, a human protein homologous to *C. elegans* CED-4, participates in cytochrome c-dependent activation of caspase-3. *Cell* 1997;90:405-413.
- 30 Green DR: Apoptotic pathways: the roads to ruin. *Cell* 1998;94:695-698.
- 31 Thornberry NA, Lazebnik Y: Caspases: enemies within. *Science* 1998;281:1312-1316.
- 32 Enari M, Talanian RV, Wong WW, Nagata S: Sequential activation of ICE-like and CPP32-like proteases during Fas-mediated apoptosis. *Nature* 1996;380:723-726.
- 33 Anversa P, Cheng W, Liu Y, Redaelli G, Kajstura J: Apoptosis and myocardial infarction. *Basic Res Cardiol* 1998;93:8-12.
- 34 Piro FR, di Gioia CR, Gallo P, Giordano C, d'Amati G: Is apoptosis a diagnostic marker of acute myocardial infarction? *Arch Pathol Lab Med* 2000;124:827-831.
- 35 Yang RY, Hsu DK, Liu FT: Expression of galectin-3 modulates T-cell growth and apoptosis. *Proc Natl Acad Sci U S A* 1996;93:6737-6742.
- 36 Fukumori T, Takenaka Y, Yoshii T, Kim HR, Hogan V, Inohara H, Shono M, Kanayama HO, Ellerhorst J, Lotan R, Raz A: CD29 and CD7 mediate galectin-3-induced type II T-cell apoptosis. *Cancer Res* 2003;63:8302-8311.
- 37 Yu F, Finley RL, Raz A, Kim HR: Galectin-3 translocates to the perinuclear membranes and inhibits cytochrome c release from the mitochondria. A role for synexin in galectin-3 translocation. *J Biol Chem* 2002;277:15819-15827.
- 38 Fukumori T, Oka N, Takenaka Y, Nangia-Makker P, Elsamman E, Kasai T, Shono M, Kanayama HO, Ellerhorst J, Lotan R, Raz A: Galectin-3 regulates mitochondrial stability and antiapoptotic function in response to anticancer drug in prostate cancer. *Cancer Res* 2006;66:3114-3119.

- 39 Garcia M1, Platet N, Liaudet E, Laurent V, Derocq D, Brouillet JP, Rochefort H: Biological and clinical significance of cathepsin D in breast cancer metastasis. *Stem Cells* 1996;14:642-650.
- 40 Minchew CL, Didenko VV: Dual Detection of Nucleolytic and Proteolytic Markers of Lysosomal Cell Death: DNase II-Type Breaks and Cathepsin D. *Methods Mol Biol* 2017;1554:229-236.
- 41 Brojatsch J, Lima H Jr., Palliser D, Jacobson LS, Muehlbauer SM, Furtado R, Goldman DL, Lisanti MP, Chandran K: Distinct cathepsins control necrotic cell death mediated by pyroptosis inducers and lysosome-destabilizing agents. *Cell Cycle* 2015;14:964-972.
- 42 Johansson AC, Appelqvist H, Nilsson C, Kågedal K, Roberg K, Ollinger K: Regulation of apoptosis-associated lysosomal membrane permeabilization. *Apoptosis* 2010;15:527-540.
- 43 Porte Alcon S, Gorojod RM, Kotler ML: Regulated Necrosis Orchestrates Microglial Cell Death in Manganese-Induced Toxicity. *Neuroscience* 2018;393:206-225.
- 44 Turk B, Stoka V: Protease signalling in cell death: caspases versus cysteine cathepsins. *FEBS Lett* 2007;581:2761-2767.
- 45 Conus S, Perozzo R, Reinheckel T, Peters C, Scapozza L, Yousefi S, Simon HU: Caspase-8 is activated by cathepsin DD initiating neutrophil apoptosis during the resolution of inflammation. *J Exp Med* 2008;205:685-698.
- 46 Aits S, Jaattela M: Lysosomal cell death at a glance. *J Cell Sci* 2013;126:1905-1912.
- 47 Oka N, Nakahara S, Takenaka Y, Fukumori T, Hogan V, Kanayama HO, Yanagawa T, Raz A: Galectin-3 inhibits tumor necrosis factor-related apoptosis-inducing ligand-induced apoptosis by activating Akt in human bladder carcinoma cells. *Cancer Res* 2005;65:7546-7553.
- 48 Datta SR, Brunet A, Greenberg ME: Cellular survival: a play in three Akts. *Genes Dev* 1999;13:2905-2927.
- 49 Christian F, Smith EL, Carmody RJ: The Regulation of NF- $\kappa$ B Subunits by Phosphorylation. *Cells* 2016;5:E12.
- 50 Mercurio F, Manning A: Multiple signals converging on NF- $\kappa$ B. *Curr Opin Cell Biol* 1999;11:226-232.
- 51 Foo SY, Nolan GP: NF- $\kappa$ B to the rescue: RELs, apoptosis and cellular transformation. *Trends Genet* 1999;15:229-235.
- 52 Ikemori RY, Machado CM, Furuzawa KM, Nonogaki S, Osinaga E, Umezawa K, de Carvalho MA, Verinaud L, Chammas R: Galectin-3 up-regulation in hypoxic and nutrient deprived microenvironments promotes cell survival. *PLoS One* 2014;9:e111592.
- 53 Dumic J1, Lauc G, Flögel M: Expression of galectin-3 in cells exposed to stress-roles of jun and NF- $\kappa$ B. *Cell Physiol Biochem* 2000;10:149-158.
- 54 Zhou W, Chen X, Hu Q, Chen X, Chen Y, Huang L: Galectin-3 activates TLR4/NF- $\kappa$ B signaling to promote lung adenocarcinoma cell proliferation through activating lncRNA-NEAT1 expression. *BMC Cancer* 2018;18:580.
- 55 Matei N, Camara J, McBride D, Camara R, Xu J, Tang J, Zhang JH: Intranasal wnt3a Attenuates Neuronal Apoptosis through Frz1/PIWIL1a/FOXO1 Pathway in MCAO Rats *J Neurosci* 2018;38:6787-6801.
- 56 Wang HS, Nie X, Wu RB, Yuan HW, Ma YH, Liu XL, Zhang JY, Deng XL, Na Q, Jin HY, Bian YC, Gao YM, Wang YD, Chen WD: Downregulation of human Wnt3 in gastric cancer suppresses cell proliferation and induces apoptosis. *Onco Targets Ther* 2016;9:3849-3860.
- 57 You Z, Saims D, Chen S, Zhang Z, Guttridge DC, Guan KL, MacDougald OA, Brown AM, Evan G, Kitajewski J, Wang CY: Wnt signaling promotes oncogenic transformation by inhibiting c-Myc-induced apoptosis. *J Cell Biol* 2002;157:429-440.
- 58 Shimura T, Takenaka Y, Fukumori T, Tsutsumi S, Okada K, Hogan V, Kikuchi A, Kuwano H, Raz A: Implication of galectin-3 in Wnt signaling. *Cancer Res* 2005;65:3535-3537.
- 59 Song S1, Mazurek N, Liu C, Sun Y, Ding QQ, Liu K, Hung MC, Bresalier RS: Galectin-3 mediates nuclear beta-catenin accumulation and Wnt signaling in human colon cancer cells by regulation of glycogen synthase kinase-3 $\beta$  activity. *Cancer Res* 2009;69:1343-1349.
- 60 Chen S, Guttridge DC, You Z, Zhang Z, Fribley A, Mayo MW, Kitajewski J, Wang CY: Wnt-1 signaling inhibits apoptosis by activating beta-catenin/T cell factor-mediated transcription. *J Cell Biol* 2001;152:87-96.
- 61 Ma B, Hottiger MO: Crosstalk between Wnt/ $\beta$ -Catenin and NF- $\kappa$ B Signaling Pathway during Inflammation. *Front Immunol* 2016;7:378.
- 62 Farnworth SL, Henderson NC, Mackinnon AC, Atkinson KM, Wilkinson T, Dhaliwal K, Hayashi K, Simpson AJ, Rossi AG, Haslett C, Sethi T: Galectin-3 reduces the severity of pneumococcal pneumonia by augmenting neutrophil function. *Am J Pathol* 2008;172:395-405.